

Low tendon stiffness and abnormal ultrastructure distinguish classic Ehlers-Danlos syndrome from benign joint hypermobility syndrome in patients

Rie Harboe Nielsen,^{*,†,1} Christian Couppé,[†] Jacob Kildevang Jensen,^{*,†} Morten Raun Olsen,^{*,†} Katja Maria Heinemeier,^{*,†} Fransiska Malfait,[§] Sofie Symoens,[§] Anne De Paepe,[§] Peter Schjerling,^{*,†} Stig Peter Magnusson,[†] Lars Remvig,^{||} and Michael Kjaer^{*,†}

*Institute of Sports Medicine, Department of Orthopaedic Surgery, and [†]Musculoskeletal Rehabilitation Research Unit, Department of Physical Therapy, Bispebjerg Hospital, Copenhagen, Denmark; [‡]Faculty of Health and Medical Sciences, University of Copenhagen, Copenhagen, Denmark; [§]Centre for Medical Genetics, University Hospital, Ghent, Belgium; and ^{||}Department of Rheumatology, Rigshospitalet, Copenhagen, Denmark

ABSTRACT There is a clinical overlap between classic Ehlers-Danlos syndrome (cEDS) and benign joint hypermobility syndrome (BJHS), with hypermobility as the main symptom. The purpose of this study was to investigate the role of type V collagen mutations and tendon pathology in these 2 syndromes. In patients (cEDS, $n=7$; BJHS, $n=8$) and controls (Ctrl, $n=8$), we measured patellar tendon ultrastructure (transmission electron microscopy), dimensions (magnetic resonance imaging), and biomechanical properties (force and ultrasonographic measurements during a ramped isometric knee extension). Mutation analyses (*COL5A1* and *COL5A2*) were performed in the patients. *COL5A1* mutations were found in 3 of 4 of the patients with cEDS. Patellar tendon dimensions were similar between the groups, but large, irregular collagen fibrils were in 4 of 5 patients with cEDS. In the cEDS group, tendon stiffness and Young's modulus were reduced to ~50% of that in BJHS and Ctrl groups ($P<0.05$). The nonhypermobility, healthy controls were matched with the patients in age, sex, body weight, and physical activity, to compare outcomes. *COL5A1* mutations led to structural tendon pathology and low tendon stiffness in cEDS, explaining the patients' hypermobility, whereas no tendon pathology was found that explained the hypermobility in BJHS.—Nielsen, R. H., Couppé, C., Jensen, J. K., Olsen, M. R., Heinemeier, K. M., Malfait, F., Symoens, S., De Paepe, A., Schjerling, P., Magnusson, S. P., Remvig, L., Kjaer, M. Low tendon stiffness and abnormal ultrastructure distinguish classic Ehlers-Danlos syndrome from benign joint hypermobility syn-

drome in patients. *FASEB J.* 28, 4668–4676 (2014). www.fasebj.org

Key Words: muscle • cauliflower fibrils • null-allele analysis

EHLERS-DANLOS SYNDROME (EDS) comprises a group of heritable connective tissue disorders characterized by joint hypermobility and tissue fragility (1, 2). The current diagnostic criteria, established in 1997 (1), subdivide EDS into 6 major types, with the 2 most common being the hypermobile (hEDS) and the classic (cEDS) types. The major diagnostic criteria for cEDS are joint hypermobility, skin hyperextensibility, and widened atrophic scarring (1). Mutations in the collagen type V-encoding genes *COL5A1* and *COL5A2* are the primary cause of cEDS; mutations in these genes have been demonstrated in > 90% of patients with cEDS who fulfilled the 3 major criteria (3). Joint hypermobility is also a major diagnostic criterion in hEDS, together with milder skin involvement and a positive family history. However, in contrast to cEDS, the causative gene is unknown and unmapped (4). Therefore, hEDS is a clinical diagnosis that can be difficult to distinguish from benign joint hypermobility syndrome (BJHS) because of the considerable overlap of clinical signs in the criteria sets (1, 5). In fact, some researchers argue that hEDS and BJHS are the same disease (4, 6). In the current study, we wanted to investigate patients with cEDS and compare them with those with BJHS with hypermobility and no skin involvement.

Abbreviations: BJHS, benign joint hypermobility syndrome; cEDS, classic Ehlers-Danlos syndrome; CSA, cross-sectional area; EDS, Ehlers-Danlos syndrome; FOV, field of view; gDNA, genomic DNA; hEDS, hypermobile Ehlers-Danlos syndrome; MRI, magnetic resonance imaging; NMD, nonsense-mediated decay; SNP, single-nucleotide polymorphism; TEM, transmission electron microscopy

¹ Correspondence: Institute of Sports Medicine, Building 8, Bispebjerg Hospital, Bispebjerg Bakke 23, 2400 Copenhagen NV, Denmark. E-mail: rieharboenielsen@gmail.com
doi: 10.1096/fj.14-249656

This article includes supplemental data. Please visit <http://www.fasebj.org> to obtain this information.

Tendons constitute a key structure for joint stability and locomotion, and since tendon tissue primarily consists of collagen fibrils, it is plausible that patients with cEDS have structural and functional abnormalities in their tendons. However, no human studies on tendon structure in patients with EDS or BJHS have been published, but transgenic *Col5a1*^{+/-} mice, which show phenotypic similarities to patients with cEDS (7), have mildly altered tendon ultrastructure with less regular collagen fibril cross-section profiles (8). Skin ultrastructure has been imaged in these transgenic mice and in patients with cEDS and, in the dermis, the collagen structure seems more severely altered than in the mouse tendons with the presence of large and highly irregular fibrils called “cauliflower” abnormalities (7, 9, 10). These irregular collagen fibrils can be the result of reduced amounts of type V collagen, since type V collagen functions as a nucleator and regulator of the lateral growth of type I collagen fibrils (1, 12). *Col5a1*^{+/-} mice also have decreased tendon stiffness, which is primarily due to a smaller tendon cross-sectional area (CSA) compared with that of control mice (8). Several case reports of patients with EDS show spontaneous tendon ruptures (13–15), which also point toward weaker tendon biomechanical properties. The notion of an altered tendon property is further supported by a recent study of the Achilles tendon that demonstrated a lower stiffness in patients with hEDS than in healthy controls (16). In contrast, spontaneous tendon ruptures have not been reported in patients with BJHS. Magnusson *et al.* (17) showed that the passive properties of the muscle–tendon unit of the hamstrings are similar in patients with BJHS and healthy controls, despite an increased range of motion in those with BJHS. This finding suggests that the underlying pathology of joint hypermobility differs between patients with cEDS and those with BJHS, but no studies have directly measured and compared tendon properties in these patients.

The purpose of this study was to investigate the structure and function of the patellar tendon in patients with cEDS and to compare the results with those in patients with BJHS and healthy, age- and sex-matched control subjects (Ctrl group). We hypothesized that the patients with cEDS, in contrast to those with BJHS, would have a type V collagen defect that would result in smaller tendons with an altered tendon ultrastructure with less regular fibrils, as well as altered tendon biomechanical properties with decreased tendon stiffness.

MATERIALS AND METHODS

Participants

We included 8 patients with the clinical diagnosis of cEDS. They fulfilled all 3 major Villefranche criteria for cEDS: joint hypermobility, skin hyperextensibility, and widened atrophic scarring (1). These patients were matched for sex, age, and self-reported physical activity level with 8 patients with BJHS

and 8 healthy Ctrl subjects. The patients with BJHS fulfilled the Brighton criteria for BJHS (5) and did not show any pathological skin signs (atrophic scarring, soft velvet skin, or hyperextensibility). Participants with a history of knee trauma were excluded from the study. The study was performed according to the Declaration of Helsinki and was approved by the Ethics Committee of the Capital Region of Denmark (H-1-2011-010). The participants gave informed consent before enrolling in the study. All were asked to refrain from strenuous exercise 48 h before the experiments.

Tendon and skin biopsies

We sampled 1 tendon biopsy from the dominant leg of each participant, just distal from the patellar apex in the midportion of the patellar tendon. The skin was anesthetized with 2 ml lidocaine (1%), and the tendon was exposed with a scalpel in a 5 mm cut under sterile conditions. The biopsies were obtained with a 14-gauge automatic needle (Bard Biopsy, Tempe, AZ, USA). The tendon samples were fixed for transmission electron microscopy (TEM) in 2% glutaraldehyde in 0.05 M sodium phosphate buffer (pH 7.2) and stored at 4°C. For skin sampling, the area was anesthetized with 2 ml lidocaine (1%), and biopsies were obtained under sterile conditions from the gluteus region with a 4 mm dermal biopsy punch needle (Miltex Inc., York, PA, USA). The skin biopsies were frozen in liquid nitrogen and stored at -80°C.

COL5A1 and COL5A2 mutation analysis

None of the patients with cEDS or BJHS had been genetically tested before the study. We used DNA from blood samples to test for mutations in the *COL5A1* and *COL5A2* genes. Since there have been reports of patients with cEDS who had *COL5A1* haploinsufficiency, but in whom the causal *COL5A1* mutation could not be identified (3), we used a skin biopsy for isolation of DNA and RNA and performed a molecular *COL5A1* allele analysis on 3 known single-nucleotide polymorphisms (SNPs) to test whether only one or both alleles were being transcribed (see next section). From whole blood, we isolated genomic DNA (gDNA) by using the Genra PureGene DNA purification kit (Qiagen, Hilden, Germany). All exons and flanking introns of the *COL5A1* and *COL5A2* genes were PCR amplified (primer sequences listed in Supplemental Data) and direct Sanger sequencing was performed on the ABI3730XL automated sequencer (Life Technologies-Applied Biosystems, Foster City, CA, USA). Mutation nomenclature follows the HGMD guidelines and nucleotide numbering corresponds to the *COL5A1* and *COL5A2* reference sequences (NM_000093.3 and NM_000393.3, respectively). The mutation was analyzed by using Alamut 2.3 software (Interactive Biosoftware, Rouen, France), which includes the *in silico* prediction tools SIFT, PolyPhen2, and MutationTaster. A mutation was considered to be pathogenic if 1 or more of the following criteria were satisfied: generation of a premature termination codon; a previously published mutation that was included in the LOVD EDS Variant Database (18); a glycine substitution in the Gly-X-Y repeat of the triple helix domain; a substitution or deletion of a cysteine residue in the C-propeptide domain; a *de novo* mutation in the index patient predicted to be deleterious by the Alamut software and absent in 105 control samples (19); genomic deletions removing part of an exon; and splice site mutations with a predicted altered splicing using Splice Site Prediction by Neural Network (20) and Human Splicing Finder software (21). Because a causal mutation was identified in the *COL5A1* gene, the *COL5A2* gene was not further investigated.

COL5A1 null-allele analysis

Skin biopsies were homogenized in 1 ml TriReagent (Molecular Research Center, Cincinnati, OH, USA) using a bead mixer with steel beads (Biospec Products, Bartlesville, OK, USA). After homogenization, bromochloropropane (Molecular Research Center) was added, to separate the samples into aqueous and organic phases, with RNA in the aqueous phase and DNA in the interphase. In addition, 80 µg glycogen was added to improve precipitation of RNA. After isolation of the aqueous phase, RNA was precipitated with isopropanol, washed in ethanol, and dissolved in RNase-free water. Total RNA concentrations were determined by spectroscopy, and good RNA quality was ensured by gel electrophoresis. Total RNA (500 ng) from each sample was converted to cDNA by reverse transcription in 20 µl with 10 µM random hexamers and Omniscript Reverse Transcriptase (Qiagen). Genomic (g)DNA was isolated from the interphase/phenol phase by extraction with 500 µl guanidine buffer (4 M guanidine-thiocyanate, 50 mM sodium-citrate, and 1 M Tris base). After vortexing and centrifuging, the aqueous phase was isolated, linear acrylamide (Molecular Research Center) was added, and the RNA was precipitated with isopropanol. After a wash with 75% ethanol, the pellet was dissolved in 100 µl 8 mM NaOH. Both cDNA and gDNA were diluted 20 times in TE, and 5 µl per reaction was used for real-time qPCR. The amplification was performed in 25 µl Quantitect SYBR Master Mix (Qiagen) with specific primers (100 nM each; **Table 1**) on a real-time PCR system (MX3005P; Stratagene, La Jolla, CA, USA). The thermal profile was 95°C, 10 min → (95°C, 15 s → 58°C, 30 s → 63°C, 90 s) × 50 → 95°C, 60 s → 55°C, 30 s → 95°C, 60 s. Signal intensity was acquired at the 63°C step, and the C_t values were related to a standard curve made with known concentrations of DNA oligos (Ultramer oligos; Integrated DNA Technologies; Leuven, Belgium) with a DNA sequence corresponding to the sequence of the expected PCR product. The specificity of the PCR products was confirmed by comparing the melting curves for the unknown samples with the melting curves of the DNA oligos after amplification (the 55→95°C step). Furthermore, primer discrimination between the 2 SNP types was ensured by comparing amplification of the correct SNP standard with the other SNP standard (≥100-fold difference). Single-nucleotide-spe-

cific primers were constructed according to the guidelines published by Wangkumhang *et al.* (22). The SNP genotypes were determined by the gDNA results, such that similar levels for both SNP versions were considered heterozygous for that SNP set. For these, the 2 cDNA results from the same sample and SNP set were compared by taking the ratio between the smaller and the larger values (corresponding to the expression ratio between each of the 2 COL5A1 alleles). If >1 SNP set was available, the average ratio was used. For all the measured cEDS samples, the ratio was close to 0.5 (0.42-0.46) and for the BJHS samples, it was close to 1 (0.83-0.96). For ease of comparison, the mean ratio of the BJHS samples was set to exactly 1, and all ratios were normalized accordingly. These ratios are given in percentages (*i.e.*, percentage expression of the weak allele *vs.* the strong allele).

TEM of tendon samples

Patellar tendon samples were postfixed in 1% OsO₄ in 0.12 M sodium cacodylate buffer (pH 7.2) for 2 h, dehydrated in a graded series of ethanols, transferred to propylene oxide, and embedded in Epon (Hexion, Houston, TX, USA) according to standard procedures. Ultrathin sections were cut with a Reichert-Jung Ultracut E microtome, collected on Formvar membranes, and stained with uranyl acetate and lead citrate. Digital images were obtained with a CM100TEM (80 kV) (Philips, Eindhoven, The Netherlands) equipped with a SIS MegaView2 camera (Olympus, Tokyo, Japan).

Magnetic resonance imaging (MRI) of the patellar tendon

The patellar tendon of the dominant leg was scanned in a 3-T MRI scanner before biopsies and biomechanical testing, to avoid tissue swelling. The tendon was visualized with an axial sequence [T1 (TR 580, TE 17), matrix 256 (0.6*0.4*3); field of view (FOV) 170, 1 NEX, slice thickness 3 mm] and a sagittal sequence [T1 (TR 650, TE 17), matrix 265 (0.8*0.6*0.4); FOV 170, 1 NEX, slice thickness 4 mm]. The scanning images were used to quantify tendon dimensions, and a blinded examiner measured 3 CSAs (proximal, middle, and distal tendon levels, reported in Results as the mean of these 3 measures) and the tendon length (software: Osirix 2.7.5,

TABLE 1. Oligonucleotides for COL5A1 null-allele testing

SNP target	Primers and standard sequence
HsCOL5A1 rs12722_C	
Primers	5'-CCACGCTCTGCCACACCCTC-3', 5'-CCCAACCCCTGAGACCTATTC-3'
Standard	5'-CCACGCTCTGCCACACCCACGCGCCCGGGAGCGGGCCATGCCTCCAGCCCCCAGCTCGCCCC ACCCATCCTGTTTCGTGAATAGGTCTCAGGGGTTGGGG-3'
HsCOL5A1 rs12722_T	
Primers	5'-CCACGCTCTGCCACACCCTC-3', 5'-CCCAACCCCTGAGACCTATTC-3'
Standard	5'-CCACGCTCTGCCACACCCATGCGCCCGGGAGCGGGCCATGCCTCCAGCCCCCAGCTCG CCCGACCCATCCTGTTTCGTGAATAGGTCTCAGGGGTTGGGG-3'
HsCOL5A1 rs3124299_C	
Primers	5'-GCACTACAGCCCTGACTGTGACAAC-3', 5'-CATCTGGATTGGGGTCCTGCGA-3'
Standard	5'-GCACTACAGCCCTGACTGTGACACCCGAGTACCTGACACCCACAGTCGCAGGACCCCAATCCAGATG-3'
HsCOL5A1 rs3124299_T	
Primers	5'-GCACTACAGCCCTGTCTGTGACAAT-3', 5'-CATCTGGATTGGGGTCCTGCGA-3'
Standard	5'-GCACTACAGCCCTGACTGTGACTGCAGTACCTGACACCCACAGTCGCAGGACCCCAATCCAGATG-3'
HsCOL5A1 rs3811146_G	
Primers	5'-TCGGGCTCATCGGTCCTCCG-3', 5'-AGACCAGGTCGCCCTTCTCA-3'
Standard	5'-TCGGGCTCATCGGTCCTCCGGTGAACAGGGTGAGAAGGGCGACCGTGGTCT-3'
HsCOL5A1 rs3811146_C	
Primers	5'-TCGGGCTCATCGGTCCTCTC-3', 5'-AGACCAGGTCGCCCTTCTCA-3'
Standard	5'-TCGGGCTCATCGGTCCTCCCGTGAACAGGGTGAGAAGGGCGACCGTGGTCT-3'

Osirix Foundation, Geneva, Switzerland). All measurements were performed 3 times, and the mean values were used.

Biomechanical testing of the patellar tendon

A schematic drawing of the test setup is shown in **Fig. 1**. Details of the measurement, including the reliability of the method in our laboratory, have been reported previously (23). The participants performed a 5 min warmup on a stationary bicycle, to ensure proper preconditioning of the tendon before testing. Subsequently, the participants were seated in a custom-made, rigid chair with both hips and knees flexed at a 90° angle. A leg cuff, which was connected to a strain gauge (Noraxon Inc., Scottsdale, AZ, USA), was mounted on the leg just above the medial malleolus. A Hitachi EUB-6500 ultrasound scanner (Hitachi Medical Corp., Tokyo, Japan) equipped with a 10 MHz, 100 mm, linear array B-mode transducer (Hitachi; Model EUP-L53L) was fitted into a custom-made, rigid cast that was secured to the skin above the patellar tendon in the sagittal plane. The ultrasound probe and cast were positioned so that the distal patella bone, the entire patellar tendon, and the proximal tibia were all visible within the FOV throughout the performed isometric ramp contractions. The participants performed 4 to 5 slow isometric knee extension ramps by applying gradually increasing force until it reached maximum over a 10 s period, during which patellar tendon displacement and knee extension force were measured simultaneously. All measurements were performed on the dominant leg. The strength of the quadriceps muscle was determined as the maximum knee extensor moment during a 10 s ramp contraction. During the ramps, ultrasound S-VHS video im-

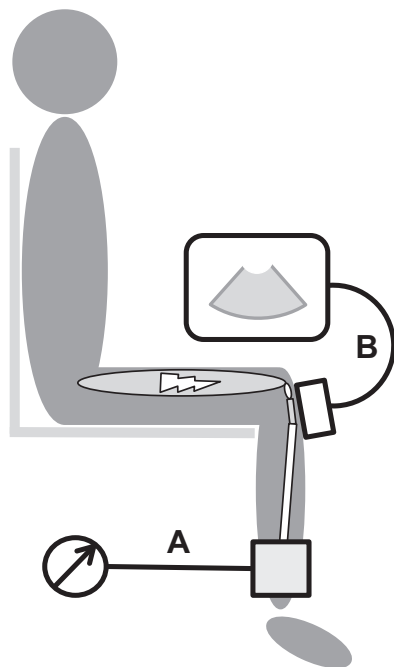


Figure 1. Test setup for the biomechanical measurements of patellar tendon properties. The subject was positioned in a rigid chair with hips and knees flexed at a 90° angle. *A*) The lower leg was fixed with a strain gauge around the ankle. *B*) An ultrasound probe was positioned over the patellar tendon, visualizing the patella, the entire tendon, and the proximal tibia. Recordings were made while the subject performed a ramped 10 s maximum isometric knee extension.

ages were sampled at 25 Hz with frame-by-frame capturing software (Morphis Dual frame grabber and Imaging Library software; Matrox Electronic Systems Ltd., Montreal, Canada). Custom-made, frame-by-frame tracking software, using a pyramidal implementation of the Lukas-Kanade optical flow estimation was used to assess the tendon deformation from the ultrasound videos. The accuracy and reproducibility of this tracking software have been assessed (24). A trigger signal (pulse generator, PG 58AA; Gould Advance, Essex, UK) initiated the recording of force and the ultrasound video, thus allowing for subsequent synchronization of recorded data, during the ramp contractions.

Calculations of patellar tendon biomechanical properties

The tibia moment arm was measured (from the leg cuff to the lateral epicondyle of the knee) to calculate the knee extensor moment. The force applied to the patellar tendon was calculated by multiplying the force production (measured with the strain gauge) by the measured knee extensor moment and dividing the result by the internal moment arm, which was estimated from individually measured femur lengths (25). Tendon deformation was defined as the change in distance between the patellar apex and the tibia (23, 24). Tendon stress was calculated by dividing tendon force with the tendon CSA (mean of proximal, middle, and distal CSA from the MRI). Tendon strain was calculated as the change in length related to the initial tendon length. Polynomial functions (2nd and 3rd order) were fitted to each single force-deformation curve. Tendon stiffness (Δ force/ Δ deformation) and Young's Modulus (Δ stress/ Δ strain) were calculated at the final 10% of the force-deformation and stress-strain curves, respectively (26). Because the maximum force differed between the groups, we also evaluated the biomechanical properties at a common force. The common force was found by matching the subjects individually on age and sex between the groups (greatest common force for pairs of 3 subjects with 1 from each group). Force-deformation and stress-strain curves for common force were then fitted, and stiffness and Young's modulus was calculated the same way as for maximum force.

Statistics

Differences in baseline characteristics and tendon dimensions between groups were analyzed with 1-way ANOVA. Biomechanical measurements were not assumed to be normally distributed and therefore were analyzed with the Kruskal-Wallis test and Dunn's *post hoc* test. Prism 6.0 (GraphPad Software Inc., San Diego, CA, USA) was used for all analyses and graphic presentations. Data are presented as means \pm SEM, and values of $P < 0.05$ indicate statistical significance.

RESULTS

Participants

There were no differences in BMI or age between the 3 groups (**Table 2**). All patients (cEDS and BJHS) fulfilled the clinical criterion of joint hypermobility, with a Beighton score (to quantify joint hypermobility) ≥ 5 (present or historical), and there were similar average Beighton scores in the cEDS and BJHS groups. None of the Ctrl subjects had hypermobility (all scores < 4).

TABLE 2. Patient characteristics

Parameter	Group		
	cEDS	BJHS	Control
Anthropometric data			
Sex	1 M, 6 F	2 M, 6 F	2 M, 6 F
Age (yr)	40 (25–61)	40 (31–53)	40 (23–70)
BMI (kg/m ²)	25 (20–28)	27 (19–36)	25 (19–37)
Type V collagen, genetic information			
<i>COL5A1/A2</i> mutations	3 of 4	0 of 5	Not measured
<i>COL5A1</i> allele expression ratio (%) ^a	50 ± 1 (n=3)	100 ± 3 (n=5)	Not measured
Tendon collagen ultrastructure cauliflower abnormalities present			
	4 of 5	0 of 5	0 of 6
Tendon biomechanics			
Deformation at max force (mm)	2.4 ± 0.2	2.5 ± 0.3	2.5 ± 0.4
Stiffness at max force (N/mm)	1608 ± 200*	3935 ± 519	4602 ± 587
Strain at max force (%)	5.9 ± 0.9	6.3 ± 0.7	6.1 ± 0.7
Modulus at max force (GPa)	0.64 ± 0.09*	1.53 ± 0.21	1.87 ± 0.22
Deformation at common force (mm)	2.2 ± 0.2	2.0 ± 0.3	1.9 ± 0.3
Stiffness at common force (N/mm)	1584 ± 165*	3390 ± 618	3061 ± 309
Strain at common force (%)	5.4 ± 0.9	5.0 ± 0.7	4.6 ± 0.7
Modulus at common force (GPa)	0.65 ± 0.08*	1.37 ± 0.28	1.26 ± 0.14

Data are presented as mean and range or mean ± SEM. ^aData shown as percentage expression of one *COL5A1* allele vs. the other. **P* < 0.05 vs. control and BJHS groups.

Two of the patients with cEDS were first-degree relatives. Two patients (1 with cEDS and 1 with BJHS) were not MRI scanned because they had surgically implanted metal in their bodies and were therefore not included in measures of tendon dimensions or in biomechanical measures related to tendon dimensions (stress, strain, and modulus). After the measurements, 1 patient with cEDS was excluded from the study because of a history of very high physical activity that could have affected his tendon's mechanical properties (27).

Genotypes

Four of the patients with cEDS and 5 with BJHS were willing to participate in the collagen type V molecular analyses. Sequencing of the *COL5A1* gene revealed a heterozygous mutation in 3 of 4 patients with cEDS: c.4706dupC in exon 62 [p.(Glu1571Argfs*53)], found in patient cEDS3, and c.4955-2A>G in intron 62, found in the 2 related patients (cEDS1 and cEDS2). The c.4706dupC mutation causes a frameshift and the generation of a premature termination codon, thereby rendering this mutant mRNA prone to degradation by nonsense-mediated mRNA decay. No *COL5A2* muta-

tions were identified. In none of the patients with BJHS was a type V collagen defect detected (Tables 2 and 3 and Fig. 2). To investigate the expression of both *COL5A1* alleles, a *COL5A1* null-allele analysis was performed. In the 3 patients with cEDS harboring a *COL5A1* mutation, lower expression of 1 allele was observed (50±1%), whereas all patients with BJHS had equal expression of both alleles (100±3%; Table 2). The expected result of the mutations would be complete loss of 1 allele due to nonsense-mediated decay (NMD). However, the consistent 50% reduction in expression of 1 allele in the 3 patients with cEDS suggests that some of the mutant *COL5A1* transcripts had escaped NMD and thus were still present inside the cell, which is consistent with findings in previous studies (28). As such, NMD could be the rate-limiting factor in determining the amount of mutant *COL5A1* transcripts. For the cEDS patient in whom no mutation was found, the *COL5A1* null-allele test was not informative because of the homozygosity of all 3 SNPs at the gDNA level. Therefore, the presence of a nonfunctional *COL5A1* allele cannot be ruled out in this patient. The result supports the previous observation that *COL5A1*

TABLE 3. Collagen V mutations and *COL5A1* allele expression ratios in patients with cEDS

Patient	Collagen V mutation	<i>COL5A1</i> allele expression ratio (%)
cEDS1	<i>COL5A1</i> c.4955-2A>G intron 62	48
cEDS2	<i>COL5A1</i> c.4955-2A>G intron 62	52
cEDS3	<i>COL5A1</i> c.4706dupC exon 62	50
cEDS4	No <i>COL5A1</i> / <i>COL5A2</i> mutations found	Noninformative analysis
cEDS5	Not analyzed	Not analyzed

Allele expression data are shown as percentage expression of the weak allele vs. the strong allele.

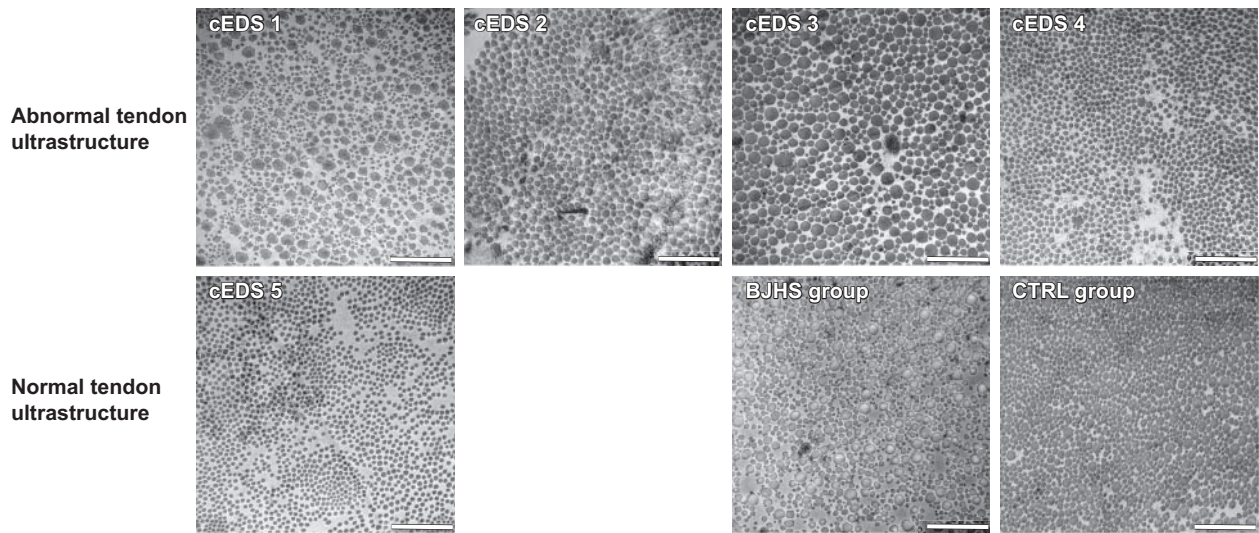


Figure 2. Patellar tendon ultrastructure. Top panels: representative images from the 4 patients with cEDS with various amounts of large and irregular collagen fibrils. See Table 3 for collagen V mutations and *COL5A1* allele expression ratios in these patients. Bottom left panel: representative image from the 5th patient with cEDS, who had normal collagen fibrils and did not undergo the allele analysis. No abnormal fibrils were found in any of the patients with BJHS ($n=5$) or in any of the control subjects (Ctrl, $n=6$); therefore, only 1 image from each group is shown as a reference. Scale bar = 1 μm .

haploinsufficiency is the most common defect in type V collagen underlying cEDS (3, 29, 30).

Patellar tendon dimensions

The dimensions of the patellar tendon were similar in all 3 groups (length: cEDS, 4.2 ± 0.3 cm; BJHS, 4.2 ± 0.2 cm, and Ctrl, 4.1 ± 0.2 cm; CSA: cEDS, 1.0 ± 0.1 cm^2 ; BJHS, 1.0 ± 0.1 cm^2 , and Ctrl, 1.0 ± 0.1 cm^2).

Patellar tendon ultrastructure

We obtained TEM images from 5 patients with cEDS, 5 with BJHS, and 6 Ctrl subjects (Fig. 2). The tendon ultrastructure in 4 of the 5 patients with cEDS revealed pathological findings of large, irregular collagen fibrils (cauliflower abnormalities, Fig. 3). These pathological fibrils were found in various amounts in the patients, always in combination with normal-appearing fibrils. The relation between the *COL5A1* mutations, *COL5A1* allele expression ratio, and tendon ultrastructure in the patients with cEDS is shown in Table 3. In the cEDS

patient in whom all fibrils appeared normal, we obtained a biopsy only from the tendon's periphery, and we could therefore have overlooked pathology in the central tendon. No abnormal collagen fibrils were found in any of the patients with BJHS or in the Ctrl subjects.

Biomechanical properties of the patellar tendon

The strain and deformation of the patellar tendon did not differ between the groups during voluntary maximum isometric knee extension. However, the produced force was significantly lower in the cEDS group compared to the Ctrl group (cEDS, 2250 ± 367 N; Ctrl, 4378 ± 629 N) but not to the BJHS group (3979 ± 557 N). The force-deformation curves are shown in Fig. 4. The slope of the last 10% of the curve (indicating tendon stiffness) was significantly lower in the cEDS group than in the BJHS and Ctrl groups (Table 2 and Fig. 4). When normalizing force and deformation to tendon dimensions, Young's modulus (tendon stiffness per area) was also found to be significantly lower in the

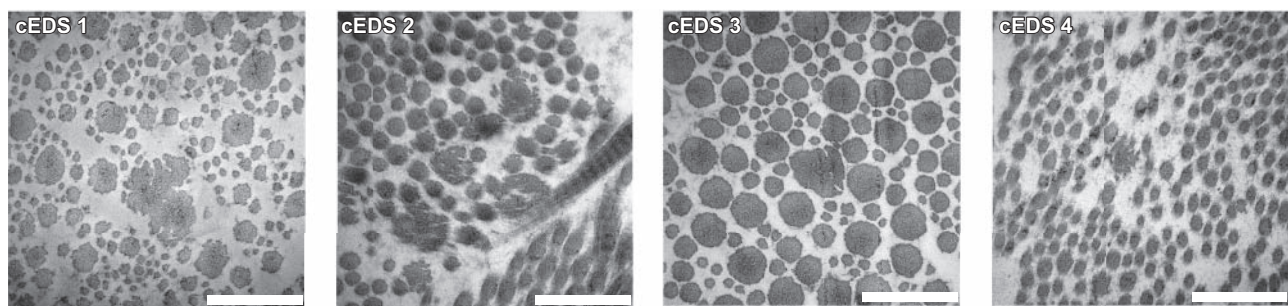


Figure 3. Patellar tendon ultrastructure abnormalities in patients with cEDS. High-magnification TEM images of cauliflower abnormalities in patellar tendon biopsies from 4 patients with cEDS. Scale bar = 0.5 μm .

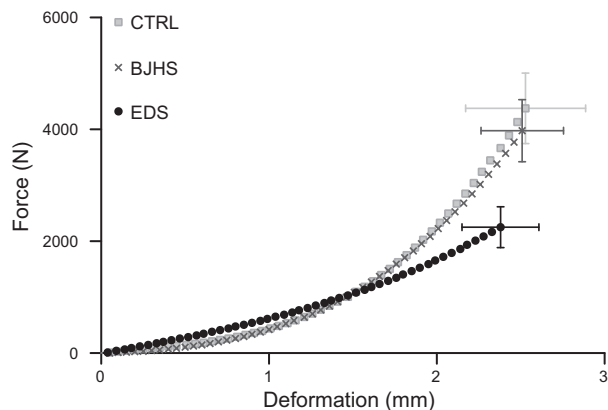


Figure 4. Force-deformation curves at maximum force. Quadriceps isometric force was applied to the patellar tendons in a ramped contraction for 10 s, to maximum voluntary force. This force is shown as a function of the corresponding tendon deformation in patients with cEDS ($n=6$), those with BJHS ($n=7$), and healthy controls (Ctrl, $n=8$). Maximum force and tendon stiffness (*i.e.*, slopes of the last 10% of the curves) were significantly lower in the cEDS group than in the BJHS and control groups. Data points are fitted mean values for the groups, with SEM shown for maximum force and deformation.

cEDS group than in the BJHS and Ctrl groups (Table 2). These severely altered tendon properties in the patients with cEDS could be due to the significantly lower muscle force produced by the patients with cEDS (although the difference in stress did not reach significance; $P = 0.06$); but also, at common force, the cEDS group had markedly lower stiffness and Young's modulus than in the BJHS and Ctrl groups (Table 2).

DISCUSSION

The main finding of this study is that the patients with cEDS had less than half the patellar tendon stiffness and Young's modulus of those with BJHS or the healthy controls. The low stiffness of the cEDS tendons was accompanied by abnormal collagen fibrils in the patellar tendons in 4 of 5 patients with cEDS and by collagen type V mutations in 3 of 4 patients with cEDS (Table 2). The prevalence of collagen V mutations in the patients with cEDS in the current study was in line with a larger scale genetic study in patients with cEDS (3). Abnormal collagen fibrils or collagen type V mutations were not detected in any of the patients with BJHS or in the healthy controls in our study.

In the current study, we observed the patellar tendon biomechanical properties in patients with cEDS and those with BJHS. Rombaut *et al.* (16) have measured Achilles tendon stiffness in patients with hEDS with similar diagnostic criteria as our BJHS group and demonstrated that the Achilles tendon stiffness was lower in patients with hEDS than in healthy controls. However, in the current study, the patients with BJHS had a patellar tendon stiffness similar to that of the healthy controls. The discrepancy between the studies could be due to methodological differences. Rombaut

et al. tracked only the movement of the proximal attachment of the Achilles tendon to the muscle, which may underestimate tendon stiffness, since it does not account for movement of the distal insertion (31). In the current study, the patellar tendon was investigated because both bony attachments can be tracked simultaneously, and consequently a more precise measure of the tendon elongation can be obtained (31). Therefore, we believe that our data provide more specific and precise measures of isolated tendon properties. In an earlier study, Magnusson *et al.* (17) were unable to demonstrate a difference in the passive tension of the muscle-tendon unit in patients with BJHS compared with that in healthy controls. The patients with BJHS in that study showed criteria similar to those with hEDS in Rombaut *et al.* (16) Some of the aforementioned discrepancies in the biomechanics of the muscle-tendon complex in patients with BJHS or hEDS may reside in the difficulty in defining and separating these diagnostic groups, which also highlights the need to develop better diagnostic tools for hEDS and BJHS.

The degree of joint hypermobility, as measured with the Beighton score, was similar in the patients with cEDS or BJHS in the current study. However, the patients with BJHS displayed much stiffer tendons than did those with cEDS. Other investigators have also observed an inconsistency between joint movement and tendon properties in healthy individuals, such that range of motion was unrelated to tendon stiffness (32). The joint hypermobility in our patients with cEDS can be explained, at least partly, by the 2-fold greater tendon compliance compared with that of the healthy controls. However, our patients with BJHS had tendon properties similar to those in the healthy controls and their joint hypermobility therefore cannot have been directly caused by tendon pathology. Joint hypermobility is seen in different heritable connective tissue disorders, such as EDS and Marfan syndrome, but also in ~10% of healthy school children (33). Therefore, it is likely that many different factors contribute to joint hypermobility. Furthermore, joint hypermobility is influenced by sex and age (33, 34) and is therefore a relatively nonspecific finding, albeit a precondition for the EDS diagnosis. We propose that measures of tendon stiffness could complement Beighton scoring in diagnosing EDS, as it adds information pertaining to the presence or absence of tendon tissue pathology.

In contrast to our hypothesis, we did not detect differences in tendon dimensions between patients and healthy controls. The lower tendon stiffness reported in *Col5a1*-haploinsufficient mice was explained by smaller tendons compared with those of wild-type mice (8); however, in the current study, the lower tendon stiffness in the patients with cEDS was caused by altered tendon material properties rather than by differences in tendon dimensions. Moreover, in contrast to the transgenic mouse model (8), the patients with cEDS in our study appeared to be more severely affected in the collagen ultrastructure of the tendon, which could explain why they displayed lower tendon stiffness per

CSA in contrast to the mouse model. The highly irregular and large collagen fibrils (cauliflower abnormalities), in combination with several normal-appearing fibrils found in our patients with cEDS, resemble the findings in skin from patients with cEDS and *Col5a1*^{+/-} mice (7, 9, 10). It is therefore likely that skin hyperextensibility and low tendon stiffness in patients with cEDS are caused by similar mechanisms. Skin hyperextensibility is part of the diagnostic criteria for cEDS, but the interexaminer agreement on the results of the clinical skin extensibility test is not particularly convincing. In fact, it has been reported to be as low as 44% (35). Different devices that measure the biomechanical properties of skin have been tried as alternatives to the manual test, but these devices are typically associated with considerable variation within the diagnostic groups, and they are not routinely used in the clinic (36, 37). Ultrasonographic *in vivo* determination of tendon mechanical properties, as used in this study, has been shown to be reproducible, with a within- and between-day correlation coefficient and typical error of 0.95 and 9.9% and 0.94 and 8.7%, respectively, for tendon stiffness (23). Thus, noninvasive measurement of tendon stiffness could be regarded as an alternative diagnostic tool to the skin extensibility test.

In summary, patients with cEDS displayed pathology in both patellar tendon structure and function, which clearly distinguished them from patients with BJHS and healthy controls. Patellar tendon ultrastructure in patients with cEDS presented with abnormal collagen fibrils similar to those previously observed in skin. Patellar tendon stiffness and Young's modulus were reduced to approximately half in patients with cEDS compared to patients with BJHS and healthy controls. These substantial differences in tendon biomechanical properties could be of interest in the diagnosis of EDS, since a noninvasive method of testing tendon mechanical properties may supplement other clinical tests (*e.g.*, Beighton score or a skin extensibility test). FJ

The authors thank C. Bøjstrup for preparation of samples, and C. E. Hansen for excellent TEM assistance, and the patients and healthy volunteers for their participation in the study. This work was supported by the Danish Rheumatism Association (R 108-A2458), a Methusalem grant from Ghent University (grant 08/01M01108), the Fund for Scientific Research FWO, Flanders, Belgium (grant G.0171.05), the Lundbeck Foundation, the Nordea Foundation, and the Novo Nordic Foundation. The authors declare no conflicts of interest.

REFERENCES

- Beighton, P., De Paepe, A., Steinmann, B., Tsipouras, P., and Wenstrup, R. J. (1998) Ehlers-Danlos syndromes: revised nomenclature, Villefranche, 1997. *Am. J. Med. Genet.* **77**, 31–37
- Beighton, P. (1972) Articular manifestations of the Ehlers-Danlos syndrome. *Semin. Arthritis Rheum.* **1**, 246–261
- Symoens, S., Sys, D., Malfait, F., Callewaert, B., De Backer, J., Vanakker, O., Coucke, P., and De Paepe, A. (2012) Comprehensive molecular analysis demonstrates type V collagen mutations in over 90% of patients with classic EDS and allows to refine diagnostic criteria. *Hum. Mutat.* **33**, 1485–1493
- Castori, M. (2012) Ehlers-Danlos syndrome, hypermobility type: an underdiagnosed hereditary connective tissue disorder with mucocutaneous, articular, and systemic manifestations. *ISRN Dermatol.* **2012**, 751768
- Grahame, R., Bird, H. A., and Child, A. (2000) The revised (Brighton 1998) criteria for the diagnosis of benign joint hypermobility syndrome (BJHS). *J. Rheumatol.* **27**, 1777–1779
- Tinkle, B. T., Bird, H. A., Grahame, R., Lavalley, M., Levy, H. P., and Silience, D. (2009) The lack of clinical distinction between the hypermobility type of Ehlers-Danlos syndrome and the joint hypermobility syndrome (a.k.a. hypermobility syndrome). *Am. J. Med. Genet.* **149**, 2368–2370
- Wenstrup, R. J., Florer, J. B., Davidson, J. M., Phillips, C. L., Pfeiffer, B. J., Menezes, D. W., Chervoneva, I., and Birk, D. E. (2006) Murine model of the Ehlers-Danlos syndrome. *col5a1* haploinsufficiency disrupts collagen fibril assembly at multiple stages. *J. Biol. Chem.* **281**, 12888–12895
- Wenstrup, R. J., Smith, S. M., Florer, J. B., Zhang, G., Beason, D. P., Seegmiller, R. E., Soslowsky, L. J., and Birk, D. E. (2011) Regulation of collagen fibril nucleation and initial fibril assembly involves coordinate interactions with collagens V and XI in developing tendon. *J. Biol. Chem.* **286**, 20455–20465
- Hausser, I., and Anton-Lamprecht, I. (1994) Differential ultrastructural aberrations of collagen fibrils in Ehlers-Danlos syndrome types I-IV as a means of diagnostics and classification. *Hum. Genet.* **3**, 394–407
- Vogel, A., Holbrook, K. A., Steinmann, B., Gitzelmann, R., and Byers, P. H. (1979) Abnormal collagen fibril structure in the gravis form (type I) of Ehlers-Danlos syndrome. *Lab. Invest.* **40**, 201–206
- Sun, M., Chen, S., Adams, S. M., Florer, J. B., Liu, H., Kao, W. W., Wenstrup, R. J., and Birk, D. E. (2011) Collagen V is a dominant regulator of collagen fibrillogenesis: dysfunctional regulation of structure and function in a corneal-stroma-specific *Col5a1*-null mouse model. *J. Cell. Science* **124**, 4096–4105
- Wenstrup, R. J., Florer, J. B., Brunskill, E. W., Bell, S. M., Chervoneva, I., and Birk, D. E. (2004) Type V collagen controls the initiation of collagen fibril assembly. *J. Biol. Chem.* **279**, 53331–53337
- Pálvölgyi, R., Bálint, B. J., and Józsa, L. (1979) The Ehlers-Danlos syndrome causing lacerations in tendons and muscles. *Arch. Orthop. Traumat. Surg.* **95**, 173–176
- Moretti, B., Notarnicola, A., Moretti, L., Garofalo, R., and Patella, V. (2008) Spontaneous bilateral patellar tendon rupture: a case report and review of the literature. *Chir. Organi Mov.* **91**, 51–55
- Iacono, V., Cigala, F., Fazioli, F., Rosa, D., and Maffulli, N. (2010) Reconstruction of chronic patellar tendon tear with allograft in a patient with Ehlers-Danlos syndrome. *Knee Surg. Sports Traumatol. Arthrosc.* **18**, 1116–1118
- Rombaut, L., Malfait, F., De Wandele, I., Mahieu, N., Thijs, Y., Segers, P., De Paepe, A., and Calders, P. (2012) Muscle-tendon tissue properties in the hypermobility type of Ehlers-Danlos syndrome. *Arthritis Care Res.* **64**, 766–772
- Magnusson, S. P., Julsgaard, C., Aagaard, P., Zacharie, C., Ullman, S., Kobayasi, T., and Kjaer, M. (2001) Viscoelastic properties and flexibility of the human muscle-tendon unit in benign joint hypermobility syndrome. *J. Rheumatol.* **28**, 2720–2725
- Dalgleish, R. (1998) The Human Collagen Mutation Database 1998. *Nucleic Acids Res.* **26**, 253–255
- Czika, W., and Berry, J. J. (2002) Using all alleles in the multiallelic versions of the SDT and combined SDT/TDT. *Am. J. Hum. Genet.* **71**, 1235–1236
- Reese, M. G., Eeckman, F. H., Kulp, D., and Haussler, D. (1997) Improved splice site detection in Genie. *J. Comput. Biol.* **4**, 311–323
- Desmet, F. O., Hamroun, D., Lalande, M., Collod-Beroud, G., Claustres, M., and Beroud, C. (2009) Human Splicing Finder: an online bioinformatics tool to predict splicing signals. *Nucleic Acids Res.* **37**, e67
- Wangkumhang, P., Chaichoompu, K., Ngamphiw, C., Ruangrit, U., Chanprasert, J., Assawamakin, A., and Tongsimma, S. (2007) WASP: a Web-based allele-specific PCR assay designing tool for detecting SNPs and mutations. *BMC Genomics* **8**, 275

23. Hansen, P., Bojsen-Moller, J., Aagaard, P., Kjaer, M., and Magnusson, S. P. (2006) Mechanical properties of the human patellar tendon, in vivo. *Clin. Biomech.* **21**, 54–58
24. Magnusson, S. P., Hansen, P., Aagaard, P., Brønd, J., Dyhre-Poulsen, P., Bojsen-Moller, J., and Kjaer, M. (2003) Differential strain patterns of the human gastrocnemius aponeurosis and free tendon, in vivo. *Acta Physiol. Scand.* **177**, 185–195
25. Visser, J. J., Hoogkamer, J. E., Bobbert, M. F., and Huijting, P. A. (1990) Length and moment arm of human leg muscles as a function of knee and hip-joint angles. *Eur. J. Appl. Physiol.* **61**, 453–460
26. Couppe, C., Hansen, P., Kongsgaard, M., Kovanen, V., Suetta, C., Aagaard, P., Kjaer, M., and Magnusson, S. P. (2009) Mechanical properties and collagen cross-linking of the patellar tendon in old and young men. *J. Appl. Physiol.* **107**, 880–886
27. Reeves, N. D., Narici, M. V., and Maganaris, C. N. (2003) Strength training alters the viscoelastic properties of tendons in elderly humans. *Muscle Nerve* **28**, 74–81
28. Malfait, F., Coucke, P., Symoens, S., Loeys, B., Nuytinck, L., and De Paepe, A. (2005) The molecular basis of classic Ehlers-Danlos syndrome: a comprehensive study of biochemical and molecular findings in 48 unrelated patients. *Hum. Mutat.* **25**, 28–37
29. Schwarze, U., Atkinson, M., Hoffman, G. G., Greenspan, D. S., and Byers, P. H. (2000) Null alleles of the COL5A1 gene of type V collagen are a cause of the classical forms of Ehlers-Danlos syndrome (types I and II). *Am. J. Hum. Genet.* **66**, 1757–1765
30. Wenstrup, R. J., Florer, J. B., Willing, M. C., Giunta, C., Steinmann, B., Young, F., Susic, M., and Cole, W. G. (2000) COL5A1 haploinsufficiency is a common molecular mechanism underlying the classical form of EDS. *Am. J. Hum. Genet.* **66**, 1766–1776
31. Kongsgaard, M., Nielsen, C. H., Hegnsvad, S., Aagaard, P., and Magnusson, S. P. (2011) Mechanical properties of the human Achilles tendon, in vivo. *Clin. Biomech.* **26**, 772–777
32. Bojsen-Moller, J., Brogaard, K., Have, M. J., Stryger, H. P., Kjaer, M., Aagaard, P., and Magnusson, S. P. (2007) Passive knee joint range of motion is unrelated to the mechanical properties of the patellar tendon. *Scand. J. Med. Sci. Sports* **17**, 415–421
33. Decoster, L. C., Vailas, J. C., Lindsay, R. H., and Williams, G. R. (1997) Prevalence and features of joint hypermobility among adolescent athletes. *Arch. Pediatr. Adolesc. Med.* **151**, 989–992
34. Larsson, L. G., Baum, J., Mudholkar, G. S., and Srivastava, D. K. (1993) Hypermobility: prevalence and features in a Swedish population. *Br. J. Rheumatol.* **32**, 116–119
35. Remvig, L., Duhn, P. H., Ullman, S., Kobayasi, T., Hansen, B., Juul-Kristensen, B., Jurvelin, J. S., and Arokoski, J. (2009) Skin extensibility and consistency in patients with Ehlers-Danlos syndrome and benign joint hypermobility syndrome. *Scand. J. Rheumatol.* **38**, 227–230
36. Pierard, G. E., Pierard, S., Delvenne, P., and Pierard-Franchimont, C. (2013) In vivo evaluation of the skin tensile strength by the suction method: pilot study coping with hysteresis and creep extension. *ISRN Dermatol.* **2013**, 841217
37. Remvig, L., Duhn, P., Ullman, S., Arokoski, J., Jurvelin, J., Safi, A., Jensen, F., Farholt, S., Hove, H., and Juul-Kristensen, B. (2010) Skin signs in Ehlers-Danlos syndrome: clinical tests and para-clinical methods. *Scand. J. Rheumatol.* **39**, 511–517

Received for publication February 5, 2014.

Accepted for publication July 14, 2014.